Supplemental Material for Electrically-Pumped Wavelength-Tunable GaAs Quantum Dots Interfaced with Rubidium Atoms

Huiying Huang,[1,2] Rinaldo Trotta,[1] Yongheng Huo, *[1,2] Thomas Lettner,[1] Johannes S. Wildmann, [1] Javier Martín-Sánchez,[1] Daniel Huber,[1] Marcus Reindl,[1] Jiaxiang Zhang,[2] Eugenio Zallo,[2,3] Oliver G. Schmidt,[2] and Armando Rastelli[1]*
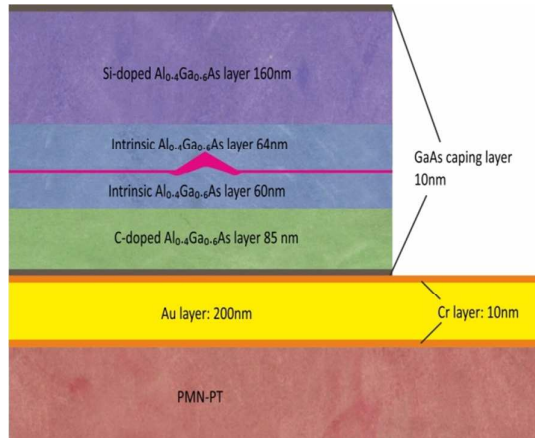
[1]Institute of Semiconductor and Solid State Physics, Johannes Kepler University, Linz, Altenbergerstraße 69, 4040, Austria

[2]Institute for Integrative Nanosciences, IFW Dresden, Helmholtzstraße 20, 01069 Germany

[3]Paul-Drude-Institut für Festkörperelektronik Hausvogteiplatz 5-7, 10117 Berlin, Germany

1. Sample structure

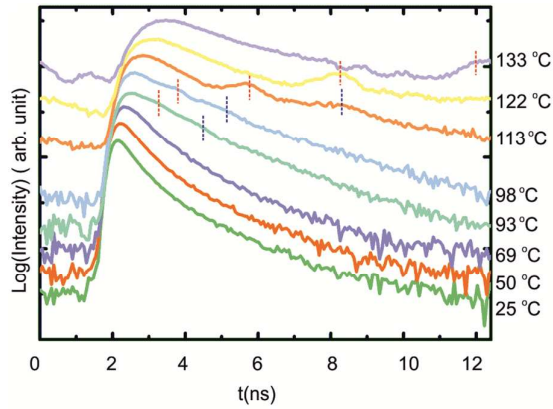The LED structure described in the text consists of the layer sequence shown in Figure S1.

Figure S1 The intrinsic Al0.4Ga0.6As/GaAs quantum dot layer is sandwiched between 160 nm-n-doped and the 85 nm-p-doped GaAs layers. A 10nm GaAs capping layer is included on both the top and bottom of the structure to prevent oxidation. After selective removal of a sacrificial layer, the resulting membrane-light-emitting-diode is intergrated on a PMN-PT substrate by Au-thermocompression-bonding. Then the device is mounted onto an AlN chip carrier providing electrical contacts both to the diode nanomembranes and the piezoelectric actuator. The n-contact on top of the membrane is done by directly contacting the n-doped semiconductor layer with an Al wire via wedge bonding.

2. Slow light for photons in resonance with Rb D2 lines

2.1 Supporting information on time delay produced by Rb cell

To support our interpretation of the delay observed in the second-order autocorrelation measurements shown in Fig.3 of the main text, we replaced the QD electroluminescence with laser pulses and recorded the arrival times of photons traversing the Rb cell at different temperatures.

A mode-locked Ti: Sapphire laser was used for this characterization. After passing the Rb cell and a monochromator (selecting a ~40 μeV-wide spectral window centered on the Rb D_2 lines), the laser pulses were sent to a single-photon detector. From the data shown in Fig. S2 we can see that the overall laser intensity decreases as the cell temperature increases. In addition there is a second maximum appearing (marked by red vertical segments), which progressively shifts towards long delay times. The second peak is ascribed to slow light for laser frequencies between the D_2 resonances. A portion of the laser spectrum falls outside the resonances and is thus not affected by the Rb gas. Due to the possible [85]Rb impurity which we will discribe later, the D_2 transition state in our cell is even more complex. Therefore, we find the third maximum (marked by black vertical segments) on Fig.S2. The intensity attenuation is caused by light absorption in the Rb cell as well as by the spread in arrival time due to dispersion. [1-3]

Figure S2 Histograms of arrival times of photons from laser-pulses after propagating through the Rb vapor cell used for the main text at different cell temperatures (measured with a temperature sensor connected with the heater). The red and black vertical segments guide the eye about the shift of the second and third maximum.

2.2 Calibration of Rb-cell temperature from transmission spectra

The temperature of the Rb cell is controlled by a proportional–integral–derivative control loop (PID controller). Due to the imperfect heat isolation, the real temperature of the Rb gas does not coincide with the temperature measured at the heater position. To determine the real temperature of the Rb vapor, we thus measured the optical transmission spectra around the Rb D_2 absorption lines at different temperatures and fit them with the simulation calculations.

2.2.1 Experimental measurement

To perform such a high resolution measurement, we sent a 15-nm-broad laser beam through a pulse-shaper with a 0.2-nm-wide transmission window and a Fabry-Perot interferometer (FPI) with a free-spectral range (FSR) of 41.4 μeV (10 GHz). The laser beam comes from a pulsed Ti: Sa-Laser with a repetition rate of 80 MHz and a typical pulse width

of the order of 100 fs. The combination of the pulse-shaper and FPI provides a theoretical resolution of 0.28 µeV. In practice, creep of the piezo-stack used in the FPI (which operates in DC mode) deteriorates the resolution. After the pulse shaper and the FPI, the beam passes though a double spectrometer with 1800 l/mm gratings (spectral resolution of ~20 µeV) and is recorded by a liquid-nitrogen-cooled CCD camera. A Lorentzian fit is applied to extract the wavelength and intensity information from the sharp FPI peaks when the FPI is scanned over the whole free spectral range. With this method, we extract the transmission spectra around Rb D_2 lines at 13 different cell temperatures, from 40 to 150 ^{o}C. From fig. S3 we can see, the D2 transmission spectra have not only two[2], but three splits. The third split indicates that, there is some ^{85}Rb impurity, which has a bit energy shift from ^{87}Rb D_2 line, inside the cell.[2,3] Theoretically, ^{85}Rb impurity should introduce two more states, but one of it, which can be found in simulation result on Fig. S3, is merged with ^{87}Rb splitting in our measurement, due to the deteriorated resolution.

2.2.2 Simulation of the transmission spectra

Since the used cell contains not only [87]Rb but, to a smaller extent, also [85]Rb atoms, we simulated the transmission of the mixture using a modified version of the "Spectra of the D_Lines of Alkali Vapors", Wolfram Demonstrations Project (Ref. 4). In this simulation the absorption coefficient κ as a function of frequency ν is calculated for the allowed transitions between the ground state $|nS_{1/2},F\rangle$ and the excited state $|n'P_{J'},F'\rangle$, where J is the total angular momentum of the electron and F the total angular momentum of the atom (including nuclear spin), using the following formula:

$$\kappa(\nu)=\frac{1}{8\pi^{3/2}}\frac{n_{at}\,3\lambda^2}{\tau\,\Delta\nu_D}\,g\left(nS_{1/2},F\to n'P_{J'},F'\right)\frac{1}{4\left(\nu\text{-}V\text{-}\nu_0\right)^2/\gamma^2+1}\exp\left[-\left(\frac{V}{\Delta\nu_D}\right)^2\right]$$

(1)

where n_{at} is the atomic density, λ the wavelength of the transition, τ the lifetime of the excited state V the velocity of the Rb atoms and $\Delta\nu_D$ the Doppler width (both normalized by λ). The latter is defined as:

$$\Delta\nu_D=\frac{1}{\lambda}\sqrt{\frac{2k_B T_{Rb}}{m_{at}}}\qquad(2)$$

where T is the vapor temperature and m_{at} the atomic mass. Furthermore the transition strengths $g\left(nS_{1/2},F\to n'P_{J'},F'\right)$ of the hyperfine components are calculate by

$$g\left(nS_{1/2},F\to n'P_{J'},F'\right)=\frac{(2J'+1)(2F+1)(2F'+1)}{2I+1}\begin{Bmatrix}1&0&1\\1/2&J'&1/2\end{Bmatrix}^2\begin{Bmatrix}J'&1/2&1\\F&F'&I\end{Bmatrix}^2\quad(3)$$

where I is the nuclear spin and the $\begin{Bmatrix}\\\end{Bmatrix}$ indicates the Racah 6j symbol.

The atomic density n_{at} is derived from the vapor pressure. The vapor pressure itself shall obey the ideal gas relations and can thus be described by the Clausius-Clapeyron law. The material specific parameter to derive the vapor pressure are taken from Refs. 2,3. Finally, the absorption $\kappa(v)$ is calculated by numerically integrating equation (1) over the velocity form $-\infty$ to ∞.

The transmission, in the end, is derived from this absorption using the Lambert-Beer law as $T=e^{-\kappa L}$, where L denotes the length of the Rubidium cell. To account for the isotope mixture of ^{85}Rb and ^{87}Rb the total absorption was calculated by adding the absorption of ^{85}Rb to the absorption of ^{87}Rb by $\kappa_{tot}=c\kappa_{85}+(1-c)\kappa_{87}$, with c as a fitting parameter.

2.2.3 Fit of the experimental data with the simulated transmission spectra

Fig. S3 presents measured transmission spectra and corresponding simulations taking the impurity concentration c and cell temperature T_{Rb} as only free parameters. In (a) we fixed the temperature T_{Rb} and varied c, while in (b) we fixed c and varied T_{Rb}. In both cases we see that the calculations do not reproduce well the measured values. We ascribe the discrepancy to errors introduced by the measurement setup (in particular the above mentioned piezo creep ot the FPI). To take into account this effect we convolve the transmission spectra with a Gaussian with linewidth Δ (GHz) and use the least square method to extract the parameters which best fit the data.
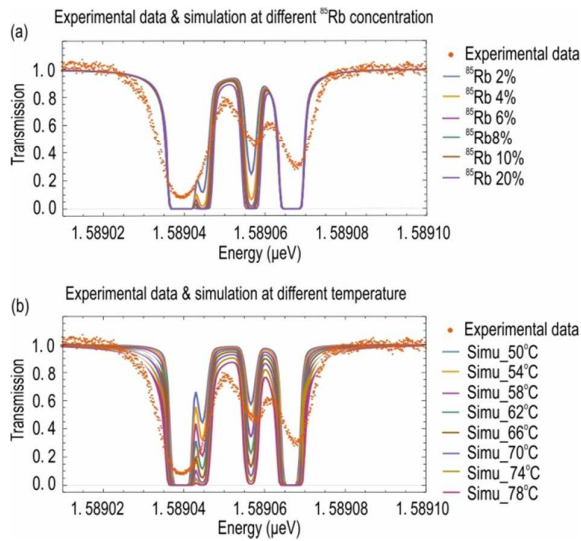
The ^{85}Rb concentration value should be the same for all the 13 measurements. The best strategy would be to find it by fitting all the 13 spectra. Since we noted that the temperature, which best fits the data, does not critically depend on the impurity value c and instrumental broadening Δ, we first determined these two parameters from the experimental data recorded at 70°C (343K). The reason for choosing the set of data collected at 70°C data is that we expect the difference between the measured and real temperature to be most pronounced at higher temperatures. Also, the transmission spectrum starts to show clear features at this temperature.

Fig. S4 (a) shows the residual (sum of the square roots of the differences between measured and simulated spectra) for Δ=0.8 GHz and ^{85}Rb concentration 4%. We see that the minimum occurs at 343 K. The simulated spectrum at this temperature is compared to the experimental data in Fig. S4 (b), showing improved agreement compared to the results obtained without Gaussian convolution. From the fitting result, we also conclude that our Rb
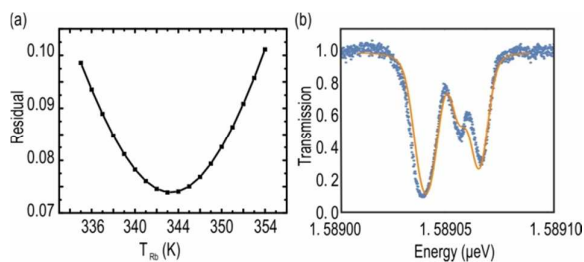
cell contains about 4% [85]Rb atoms. Fig. S5 shows the fitting results of all 13 measurements, i.e. the fitted Rb cell temperatures (a) and the corresponding residuals (b).

We see that, while the measured temperature is close to the calculated temperature up to about 80°C, pronounced deviations are apparent at higher temperatures. We attribute this observation to heat losses, which are more pronounced at higher temperatures.
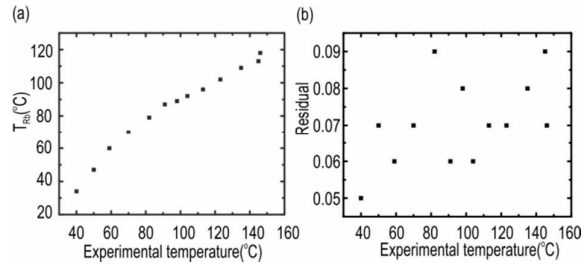

Figure S3 Measured transmission spectrum at 70°C (orange dots) and simulation results in (a) fixed cell temperature and various impurity concentration values, (b) fixed impurity and various cell temperatures.

Figure S4 (a) Residual (sum of the squared root differences between simulated and measured spectra) for Δ=0.8GHz and [85]Rb impurity= 4% as a function of simulated. (b) Final fitted plot

(orange line) as Δ=0.8GHz ,[85]Rb impurity= 4%, temperature=343K (70°C) compared with the

data (blue dot line).

Figure S5 the fitted Rb cell temperatures T_{Rb} (a) and the corresponding residuals (b) for all

the 13 measurements.

References

1. Wildmann, J. S.; Trotta, R.; Martín-Sánchez, J.; Zallo, E.; O'Steen, M.; Schmidt, O. G.; Rastelli, A. Atomic clouds as spectrally selective and tunable delay lines for single photons from quantum dots. *A. Phys. Rev. B* **2015**, 92 (23).

2. Steck, D. A. Steck. Rubidium ^{87}D Line Data.

3. Steck, D. A. Steck. Rubidium ^{85}D Line Data.

4. Gianni Di Domenico and Antoine Weis *Spectra of the D_Lines of Alkali Vapors* from the Wolfram Demonstrations
Project :http://demonstrations.wolfram.com/SpectraOfTheDLinesOfAlkaliVapors/